The Iron-Sulfur Cluster of Iron Regulatory Protein 1 Modulates the Accessibility of RNA Binding and Phosphorylation Sites†

Kevin L. Schalinske,‡ Sheila A. Anderson,‡ Polygena T. Tuazon,§ Opal S. Chen,‡ M. Claire Kennedy,|| and Richard S. Eisenstein*,‡

Department of Nutritional Sciences, University of Wisconsin—Madison, Madison, Wisconsin 53706-1571, Department of Biochemistry, University of California—Riverside, Riverside, California 92521-0129, and Department of Biochemistry, Medical College of Wisconsin, Milwaukee, Wisconsin 53226

Received September 27, 1996; Revised Manuscript Received January 15, 1997⊗

ABSTRACT: Iron regulatory protein 1 (IRP1) modulates iron metabolism by binding to mRNAs encoding proteins involved in the uptake, storage, and metabolic utilization of iron. Iron regulates IRP1 function by promoting assembly of an iron-sulfur cluster in the apo or RNA binding form, thereby converting it to the active holo or cytoplasmic aconitase form. In continuing our studies on phosphoregulation of IRP1 by protein kinase C (PKC), we noted that the purified apoprotein was more efficiently phosphorylated than was the form partially purified from liver cytosol by chromatography on DEAE-Sepharose which had characteristics of the [3Fe-4S] form of the protein. RNA binding measurements revealed a 20-fold increase in RNA binding affinity and a 4−5-fold higher rate of phosphorylation after removal of the Fe-S cluster from the highly purified [4Fe-4S] form. Phosphorylation of apo-IRP1 by PKC was specifically inhibited by IRE-containing RNA. The RNA binding form had a more open structure as judged by its much greater sensitivity to limited cleavage by a number of proteases. N-Terminal sequencing of chymotryptic peptides of apo-IRP1 demonstrated an increased accessibility to proteolysis of sites (residues 132 and 504) near or within the putative cleft of the protein, including regions that are thought to be involved in RNA binding (residues 116−151) and phosphoregulation (Ser 138). Enhanced cleavage was also observed in the proposed hinge linker region (residue 623) on the surface of the protein opposite from the cleft. Taken together, our results indicate that significant structural changes occur in IRP1 during cluster insertion or removal that affect the accessibility to RNA binding and phosphorylation sites.

Iron is an essential nutrient that is required for a number of cellular and organismal processes. However, excessive accumulation of iron can be toxic, primarily because of its ability to catalyze formation of reactive oxygen intermediates, which in turn can damage proteins, lipids, and nucleic acids (Eisenstein et al., 1997; Hentze & Kühn, 1996; Klausner et al., 1993; Theil, 1994). Consequently, the regulation and maintenance of iron homeostasis is important to ensure that adequate levels of iron are available for metabolic functions yet prevent the potentially toxic effects of excessive levels of the mineral.

Cellular iron homeostasis is modulated and maintained through changes in synthesis of proteins involved in the uptake (transferrin receptor, TfR),[1] storage (H- and L-ferritin), and utilization (erythroid 5-aminolevulinate synthase, eALAS) of this essential mineral. Synthesis of these proteins is post-transcriptionally regulated through the action of cytosolic RNA binding proteins termed iron regulatory proteins (IRPs). IRPs bind to iron responsive elements (IREs) which are stem−loop structures present in the 5′ untranslated region (UTR) of ferritin and eALAS mRNAs and in the 3′UTR of TfR mRNA. Formation of the IRP−IRE complex results in the repression of translation of ferritin and possibly eALAS mRNAs as well as the simultaneous stabilization of TfR mRNA and consequent increase in TfR synthesis. It is largely in this manner that the coordinated but divergent regulation of ferritin and TfR synthesis is linked to cellular iron status. Thus, IRPs and IREs are components of a sensory and regulatory network that ensures adequate iron uptake when iron concentrations are low and also promotes the safe sequestration of iron when its levels increase.

Two IRPs have been characterized, IRP1 and IRP2, which display similar affinities for known IREs but differ in the means by which iron affects their function (Guo et al., 1994, 1995; Hirling et al., 1994; Iwai et al., 1995; Pantopoulos et al., 1995; Philpott et al., 1993; Samaniego et al., 1994). Iron modulates the rate of degradation of IRP2 (Guo et al., 1995; Iwai et al., 1995). In contrast, IRP1 is a bifunctional protein, and iron can directly affect its binding affinity for IREs by inducing a conversion from the RNA binding form into the

† Supported in part by NIH Grant R29 DK-47219, USDA CSRS Grant 94-37200-0361, a grant from the Graduate School and College of Agricultural and Life Sciences (R.S.E.), USDA Grant 93-37200-8816 (K.L.S.), NIH Grant R01GM51831 (M.C.K.), and NIH Grant R01 GM26738 (P.T.T.). We acknowledge the use of instrumentation at the National Biomedical ESR Center (NIH Research Resources Grant RR01008) at the Medical College of Wisconsin.

* To whom correspondence should be addressed: Department of Nutritional Sciences, University of Wisconsin—Madison, 1415 Linden Drive, Madison, WI 53706-1571. Telephone: 608-262-5830. Fax: 608-262-5860. E-mail: eisenste@nutrisci.wisc.edu.

‡ University of Wisconsin—Madison.

§ University of California—Riverside.

|| Medical College of Wisconsin.

⊗ Abstract published in *Advance ACS Abstracts,* March 15, 1997.

[1] Abbreviations: TfR, transferrin receptor; IRP, iron regulatory protein; IRE, iron responsive element; eALAS, erythroid 5-aminolevulinate synthase; PMA, phorbol 12-myristate 13-acetate; PKC, protein kinase C; 2-ME, 2-mercaptoethanol; SDS−PAGE, sodium dodecyl sulfate−polyacrylamide gel electrophoresis; cDNA, complementary DNA; m-aconitase, mitochondrial aconitase; c-aconitase, cytosolic aconitase.

S0006-2960(96)02444-0 CCC: $14.00

cytoplasmic isoform of the iron-sulfur protein aconitase (c-aconitase) (Emery-Goodman et al., 1993; Haile et al., 1992a,b; Hirling et al., 1994; Kaptain et al., 1991; Kennedy et al., 1992; Philpott et al., 1993). Formation or destruction of the Fe-S cluster provides a means by which iron can modulate the genetic function of IRP1 without altering the total level of the protein. The presence of a [4Fe-4S] cluster (active holoprotein) confers aconitase activity, whereas the iron-free form (apoprotein) exhibits high affinity for IRE-containing RNAs. On the basis of its primary amino acid sequence coupled with computer predictions, it has been suggested that the tertiary structure of IRP1 is similar to mitochondrial aconitase (m-aconitase) (Hentze & Argos, 1991; Klausner et al., 1994; Rouault et al., 1991). The crystal structure of m-aconitase revealed that it contains four domains in which domains 1−3 are joined to domain 4 by a hinge linker region (Robbins & Stout, 1989). The Fe-S cluster is present in a solvent-filled cleft that is formed between domains 1−3 and domain 4. In the case of IRP1, it has been hypothesized that structural changes in the protein, which may be associated with the presence or absence of the Fe-S cluster, affect the relative degree to which the cleft is open and available for interaction with RNA (Klausner et al., 1994).

Evidence supporting the hypothesis that regulated accessibility of amino acid residues within the cleft performs a central role in the regulation of IRP1 function comes from several approaches. First, some residues that are predicted to be in the cleft are involved in RNA binding or its regulation. Of particular interest is the demonstration of the dual function of certain Cys or Arg residues in relation to the RNA binding and aconitase activities of IRP1 (Hirling et al., 1994; Philpott et al., 1993, 1994). Second, UV cross-linking coupled with protein sequencing as well as a scanning mutagenesis approach have identified residues 116−151 as being essential for RNA binding (Basilion et al., 1994; Neupert et al., 1995), and it is clear that other regions of IRP1 such as residues 480−623 can also interact with RNA (Swenson & Walden, 1994). Third, on the basis of the crystal structure of m-aconitase in the iron-loaded form, the proposed cleft in c-aconitase would not be open sufficiently to accommodate an IRE stem−loop in the active site (Klausner et al., 1994; Robbins & Stout, 1989). Taken together, this suggests that significant structural changes take place during the interconversion between the apo- and holoprotein form of IRP1 which result in a modulation of the affinity of the RNA−protein interaction.

We have recently reported that the function of IRPs can be phosphoregulated by protein kinase C (Eisenstein et al., 1993; Schalinske & Eisenstein, 1996). Phorbol 12-myristate 13-acetate (PMA)-induced stimulation of phosphate incorporation into IRP1 and IRP2 in HL60 cells resulted in an increase in RNA binding activity by both binding proteins and a concomitant elevation in TfR mRNA level (Schalinske & Eisenstein, 1996). On the basis of *in vitro* phosphorylation of both intact IRP1 and synthetic peptide fragments of the protein, Ser 138 and Ser 711 were identified as sites where PKC could act (Eisenstein et al., 1993). Because sequence homology with m-aconitase suggested that Ser 138 and Ser 711 are near the entrance to the putative cleft, we suggested that phosphorylation of IRP1 by PKC might serve as a determinant of whether the protein functions as an aconitase or an RNA binding protein. Furthermore, the recent identification of amino acids 116−151 as being essential for RNA binding (Neupert et al., 1995) provides further support for the potential role of PKC-dependent phosphorylation, particularly of Ser 138, as a determinant of IRP1 function.

Because Ser 138 and Ser 711 are predicted to be near the entrance to the putative cleft in IRP1, our goal was to examine whether differences existed in the ability of IRP1 and c-aconitase to be phosphorylated by PKC in order to further elucidate the role of phosphorylation on function. First, we demonstrate that *in vitro* IRP1[2] is a much preferred substrate for phosphorylation by PKC and displays greater affinity for binding RNA as compared to c-aconitase. Second, using limited proteolysis as a probe of protein structure, we show that the IRP1 displays much greater sensitivity to a variety of proteases as compared to c-aconitase and that sites of cleavage in the two proteins differ significantly. Third, amino acid sequencing of peptide digests of IRP1 demonstrates that residues near the entrance to and within the putative cleft as well as in the proposed hinge linker region become accessible to proteases after the Fe-S cluster is removed. Fourth, one of the sites of chymotryptic cleavage in IRP1, but not in c-aconitase, is within the area of the binding protein known to be essential for RNA binding and is also proximal to Ser 138. Fifth, IRE-containing RNA specifically inhibits phosphorylation of IRP1 by PKC. Taken together, our results demonstrate significant structural differences in IRP1 as a function of the presence or absence of the Fe-S cluster and support the hypothesis that phosphorylation by PKC serves as a molecular determinant of whether IRP1 functions as an RNA binding protein or an aconitase.

MATERIALS AND METHODS

Materials. Materials and reagents were obtained from these sources: radioactive compounds, DuPont NEN; T7 RNA polymerase, New England Biolabs; RQ1 DNase and RNasin, Promega; 2-mercaptoethanol (2-ME), Fluka; and proteases, Boehringer Mannheim.

Protein Purification. To purify IRP1, rat liver cytosol was fractionated by DEAE-Sepharose chromatography and the nonabsorbant fraction was purified to apparent homogeneity by RNA affinity chromatography using the first 73 nucleotides (nt) of the rat L-ferritin 5′UTR.[3] Under the conditions used here, IRP2 is not present in the DEAE-NA fraction (Barton et al., 1990; Guo et al., 1994). Bovine liver c-aconitase was purified as described (Kennedy et al., 1992). The apo form of bovine c-aconitase (IRP1) was prepared from the holo form by oxidation with a molar excess of ferricyanide/EDTA (oxidized IRP1) followed by gel filtration and reduction with DTT (Kennedy et al., 1992).

In Vitro Phosphorylation Assays. Semipurified or purified preparations of the apo- or holoprotein forms of IRP1 were incubated with [γ-^{32}P]ATP, bovine brain protein kinase C, buffer components, and activators of the kinase as described

[2] IRP1 or "apoprotein" refers to the form of the binding protein lacking an Fe-S cluster and capable of binding RNA with high affinity. Active cytoplasmic aconitase refers to the form of the protein with a [4Fe-4S] cluster, and "holoprotein" refers to c-aconitase with either the [3Fe-4S] or the [4Fe-4S] cluster (Beinert & Kennedy, 1993).

[3] R. S. Eisenstein, H. A. Barton, W. H. Pettingell, Jr., and A. B. Bomford, submitted for publication.

(Tuazon et al., 1989). Reactions were terminated with nonlabeled ATP and the reaction mixtures analyzed by SDS−PAGE (Eisenstein et al., 1993; Tuazon et al., 1989). Incorporation of ^{32}P into IRP1 was quantified as described (Tuazon et al., 1989).

For determination of the effects of RNA on the PKC-dependent phosphorylation of IRP1 (0.9 μg), kinase reactions were performed at 30 °C for 15 min with 3 units of PKC as described above with the addition of [^{3}H]RNA at the indicated concentrations and the ribonuclease inhibitor RNAsin at 1 unit/μL. The order of addition of the reaction components was as follows: RNA, IRP1 in kinase buffer with RNAsin, PKC activators, and PKC. Reactions were initiated by addition of [γ-^{32}P]ATP (Tuazon et al., 1989). RNA competitors were synthesized in the presence of each ribonucleotide triphosphate (all 0.5 mM) plus a trace amount of [^{3}H]UTP to permit quantitation of the yield and concentration of RNA (Bettany et al., 1992). RNAs were purified through a 10% polyacrylamide/8 M urea gel before quantitation as described (Eisenstein et al., 1993). The competitor RNAs synthesized were the first 73 nt of the rat L-ferritin 5′UTR and a secondary structure mutant of this RNA, termed 5′M, in which the 5′ side of the upper stem of the IRE no longer is able to base pair with the 3′ side of the stem (Bettany et al., 1992).

RNA Binding Analysis. RNA binding assays were performed using purified bovine liver IRP1 or c-aconitase and a gel-purified synthetic [^{32}P]IRE-containing RNA composed of the first 73 nt of the rat L-ferritin 5′UTR, as described (Barton et al., 1990; Eisenstein et al., 1993). Following a 10 min incubation period at room temperature, free and bound RNA were separated using 4% nondenaturing polyacrylamide gels. After the gels were dried, bands representing free and bound RNA were quantified as described (Barton et al., 1990; Eisenstein et al., 1993). For determination of K_D and B_{max}, purified protein was incubated with concentrations of [^{32}P]RNA ranging from 10 pM to 100 nM. To determine binding affinity and capacity under equilibrium conditions, the various protein species were added at a concentration close to their estimated binding affinities (Barton et al., 1990). Thus, c-aconitase and oxidized IRP1 were included at a concentration of 1 nM, whereas reduced IRP1 was included at 0.1 nM. B_{max} and K_D were determined by curve fitting the data using nonlinear regression (GraphPAD, San Diego, CA).

Partial Proteolytic Digestion of IRP1 and Sequencing of IRP1 Peptides. Purified c-aconitase and IRP1 (4 μg each) were digested with chymotrypsin, endo Lys-C, endo Glu-C, or endo Arg-C for varying periods of time ranging from 15 s to 30 min. Chymotrypsin [0.15 μg/(μg of IRP1)] and endo Lys-C [1.75 μg (260 mu)/(μg of IRP1)] digestions were performed in freshly prepared 20 mM Hepes (pH 7.5), 1 mM sodium citrate, and 7 mM 2-ME. Endo Glu-C digestions [1.25 μg (275 mu)/(μg of IRP1)] were in 40 mM ammonium bicarbonate (pH 7.8), 7 mM 2-ME, and 1 mM sodium citrate. Endo Arg-C [1.25 μg/(μg of IRP1)] digestions were performed in 50 mM Tris (pH 8.0), 10 mM $CaCl_2$, 5 mM EDTA, 1 mM DTT, and 1 mM sodium citrate. Following incubation at 4 °C for the indicated period of time, 10 μL of sample was withdrawn and mixed with an equal volume of reducing sample buffer (Laemmli, 1970) followed by denaturation at 100 °C for 5 min. Intact IRP1 was separated from digested products using a 12% SDS−PAGE.

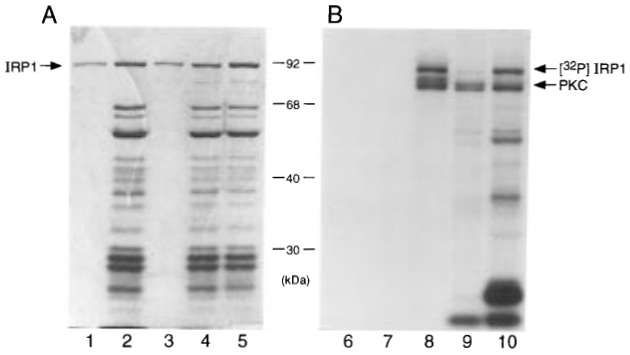

FIGURE 1: Purification of IRP1 from rat liver unmasks protein kinase C phosphorylation sites. The ability of IRP1 to serve as a substrate was determined using affinity-purified IRP1, a partially purified preparation of IRP1 composed of the nonadherent fraction from DEAE-Sepharose chromatography of rat liver cytosol and the purified IRP1 added to the DEAE-NA fraction. The highest-molecular weight polypeptide in the DEAE-NA fraction was judged to be IRP1 because (i) it comigrated with the affinity-purified binding protein (compare lanes 1 and 2) and (ii) the N-terminal 47 amino acids of the purified protein matched the sequence predicted from the cDNA sequence of rat IRP1[3] (Yu et al., 1992). Phosphorylation assays using protein kinase C were performed as described in Materials and Methods. In panel A, lanes 1−5 are a Coomassie-stained SDS polyacrylamide gel, and in panel B, lanes 6−10 depict an autoradiogram of the same gel: lanes 1 and 6, purified IRP1 (0.6 μg); lanes 2 and 7, DEAE-NA fraction (10 μg); lanes 3 and 8, purified IRP1 (0.6 μg) plus PKC (see Materials and Methods); lanes 4 and 9, DEAE-NA fraction (10 μg) plus PKC; and lanes 5 and 10, DEAE-NA (10 μg) plus purified IRP1 (0.6 μg) plus PKC. The positions of IRP1 and PKC are indicated.

Following electrophoresis, gels were fixed, stained with Coomassie Brillant Blue R250, and destained. Chymotryptic peptides were transferred from SDS gels to Immobilon PSQ PVDF membranes (Millipore), stained with Coomassie, and excised. Peptide sequencing by Edman degradation on a Applied Biosystems 477A protein sequencer was performed by the Department of Physiology at Tufts University.

RESULTS

Purification of IRP1 Unmasks PKC Phosphorylation Sites. We have reported previously that purified IRP1 is an efficient substrate for PKC as it exhibited a high stoichiometry of phosphorylation [0.5−1.3 mol of phosphate/(mol of protein)] and a low K_M (0.5 μM) (Eisenstein et al., 1993). However, we subsequently found that the ability of IRP1 to serve as a substrate for phosphorylation by PKC was altered during its purification from rat liver cytosol. Figure 1 depicts a Coomassie-stained gel (panel A) and autoradiogram (panel B) of partially purified and purified rat liver IRP1 that were used for *in vitro* phosphorylation assays. IRP1 was purified (Figure 1, lane 1) by RNA affinity chromatography of the nonadherent fraction (DEAE-NA) obtained from DEAE-Sepharose chromatography of liver cytosol (Figure 1, lane 2). Upon addition of PKC, purified IRP1 (Figure 1, lane 3) became highly phosphorylated (Figure 1, lane 8). In contrast, when PKC was added to the DEAE-NA fraction, little phosphorylation of IRP1 was observed (Figure 1, lane 9). Addition of purified IRP1 to the DEAE-NA fraction (Figure 1, compare lanes 4 and 5) resulted in a level of phosphorylation of IRP1 similar to that obtained with the pure protein itself (Figure 1, compare lanes 10 and 8). No phosphorylation was observed in these preparations of IRP1 in the absence of PKC (Figure 1, lanes 6 and 7). These results

Table 1: Characteristics of IRE RNA Binding Activity in the DEAE-NA[a,b] Fraction

basal activity[c]	+2-ME (2%) [pmol of RNA bound/(mg of protein)]	+2-ME (+citrate) [pmol of RNA bound/(mg of protein)]	+2-ME (+*cis*-aconitate) [pmol of RNA bound/(mg of protein)]
1.65 ± 0.30	6.71 ± 0.18	1.27 ± 0.24	1.41 ± 0.26

[a] This refers to the protein fraction that did not absorb to the DEAE column when rat liver cytosol was applied. [b] This fractionation was performed in the absence of citrate. [c] IRE RNA binding activity was determined by RNA gel shift analysis as indicated in Materials and Methods.

indicate that IRP1 present in the DEAE-NA fraction was in a form wherein the phosphorylation sites were largely inaccessible to PKC and purification of IRP1 converted it to a form that could be efficiently phosphorylated.

Several lines of evidence indicated that the DEAE-NA and purified forms of IRP1 differed with respect to the state of the Fe-S cluster. First, the IRE RNA binding activity of the DEAE-NA fraction was low-affinity (K_D = 1.1 nM) and required high levels (2%) of 2-ME for full activation, and aconitase substrates fully blocked the 2-ME effect (Table 1). These are properties of the [3Fe-4S] and [4Fe-4S] form of IRP1, both of which bind substrate (Beinert & Kennedy, 1993; Haile et al., 1992b; Kennedy et al., 1992). In this context, it is important to note that citrate had no effect on the 2-ME-dependent stimulation of RNA binding by the apoprotein (Haile et al., 1992b) (see Figure 3). Therefore, the 4-fold increase in RNA binding activity of the DEAE-NA fraction by 2-ME, which was totally blocked by substrate, suggests that at least 75% of the binding protein in this fraction is in the 3Fe and/or 4Fe form. Second, addition of iron and DTT, without added sulfide, stimulated aconitase activity in the DEAE-NA fraction by 100-fold (results not shown). Thus, under the conditions used for its preparation, the DEAE-NA fraction contained very little of the [4Fe-4S] form of c-aconitase.[4] Furthermore, inclusion of sulfide with the iron and DTT did not lead to a further significant increase in aconitase activity, confirming that the [3Fe-4S] species was the predominant form of the protein in the untreated DEAE-NA fraction. Third, EPR spectroscopy at 10 K of the DEAE-NA fraction gave a spectrum identical to that of the [3Fe-4S] form of c-aconitase (not shown) (Beinert & Thomson, 1983; Kennedy et al., 1992). Quantitation of the EPR signal gave a concentration of the 3Fe form of the protein that was between 80 and 100% of the amount of protein calculated to be present in the DEAE-NA extract on the basis of the enzyme activity measured after reconstitution of the 4Fe form with iron/DTT, assuming a specific activity of 4 units/(nmol of cluster) (Kennedy et al., 1992). Thus, in the DEAE-NA fraction, IRP1 was largely in the [3Fe-4S] form.

In contrast, IRP1 purified from the DEAE-NA fraction was in the apoprotein form. The pure protein lacked iron,[5] bound RNA with high affinity (K_D = 0.045 pM), and required low levels of 2-ME or DTT for activation of the RNA binding function (results not shown). These are properties of the apoprotein (Beinert & Kennedy, 1993; Haile et al., 1992b). Our results indicate that the conditions used to bind (2% 2-ME) and elute (1 M NaCl) IRP1 from the RNA affinity column under aerobic conditions led to destruction of the cluster. Taken together, these results indicate that the [3Fe-4S] form of c-aconitase is a significantly less efficient substrate for PKC-dependent phosphorylation as compared to the apoprotein form, IRP1.

RNA Binding and Phosphorylation Characteristics of Purified Forms of Bovine IRP1. Because the presence or absence of an iron-sulfur cluster in IRP1 is a determinant of whether it functions as an aconitase or RNA binding protein in intact cells, we wished to further evaluate the relationship between cluster status and phosphorylation potential. Highly purified preparations of the apo and [4Fe-4S] form of IRP1 allowed us to determine if the low phosphorylation potential of the DEAE-NA form of rat liver IRP1 was due to an inherent property of the holoprotein or to the presence of other proteins in the nonabsorbent fraction from the DEAE column. The RNA binding characteristics were determined on three forms of IRP1: [4Fe-4S], oxidized apo-, and reduced apoprotein. We used highly purified preparations of IRP1 and c-aconitase to ensure that we were using representative functional forms of the binding protein and because the affinity of interaction and/or binding capacity has not been determined for these forms of the protein.

We initially focused on the reduced IRP1 and the c-aconitase form as they appear to represent the form of IRP1 present in iron-depleted (desferal) and iron-treated (hemin) cells, respectively (Haile et al., 1992b). Gel shift analysis demonstrated that reduced IRP1 bound the IRE from rat L-ferritin mRNA with a K_D of 0.11 ± 0.02 nM and a B_{max} of 2.36 ± 0.12 nmol/(mg of protein) (Figure 2A). On the basis of the B_{max} value and assuming that one RNA molecule binds per protein molecule (Müllner et al., 1989), 26% of reduced IRP1 bound to RNA under these conditions. The c-aconitase form from bovine liver bound RNA with a K_D of 2.23 ± 0.65 nM and a B_{max} of 0.79 ± 0.04 nmol/(mg of protein) (Figure 2B). Under these conditions, 8% of c-aconitase bound to RNA. The RNA binding analyses of c-aconitase were performed in the presence of 2 mM citrate to protect the Fe-S cluster.

The RNA binding activity of IRP1 and particularly c-aconitase was stimulated by 2-ME. Addition of 10−50 mM 2-ME stimulated RNA binding by reduced IRP1 by 30%, suggesting that the protein had not been fully reduced by DTT or that it became partially oxidized under the conditions of the gel shift assay if reductant was not included (Figure 3A). In the presence of 2-ME, we observed that 33% of apo-IRP1 bound RNA, a level of active protein similar to what others have observed with IRP1 purified from numerous sources using a variety of methods (Neupert et al., 1990; Rouault et al., 1989; Walden et al., 1989; Yu et al., 1992). As noted by others, c-aconitase displayed different requirements for 2-ME activation of its RNA

[4] The [3Fe-4S] form of c-aconitase present in the DEAE-NA fraction probably arose during preparation and fractionation of cytosol since we found that inclusion of citrate in all buffers, which is known to protect the [4Fe-4S] cluster of m- and c-aconitases from oxidative destruction (Haile et al., 1992b; Kennedy et al., 1983, 1992), increased the recovery of aconitase activity in the DEAE-NA fraction to 68% of that present in the homogenate. This represented a 17-fold increase in recovery of aconitase activity as compared to fractionation in the absence of citrate (results not shown).

[5] R. S. Eisenstein, D. Wright, W. H. Orme Johnson, and H. N. Munro, unpublished observations.

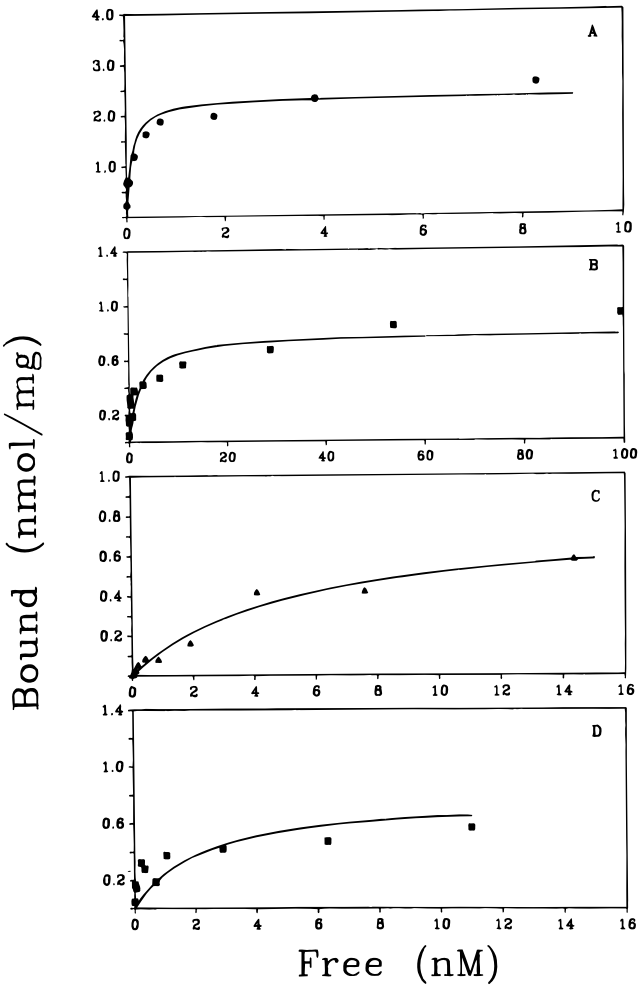

FIGURE 2: Effect of cluster status and cysteine oxidation state on RNA binding characteristics of IRP1. Measurements of equilibrium binding affinity (K_D) and capacity (B_{max}) by gel retardation assays were performed using highly purified protein and [^{32}P]RNA as indicated in Materials and Methods: (A) reduced IRP1, (B) c-aconitase, (C) oxidized IRP1, and (D) c-aconitase data replotted over the same range of RNA concentrations as was used with the oxidized IRP1. Values described in the text for K_D and B_{max} are from data that are mean ± SEM for $n = 7-9$ determinations with representative graphs shown. Note the difference in the RNA concentration for the different panels.

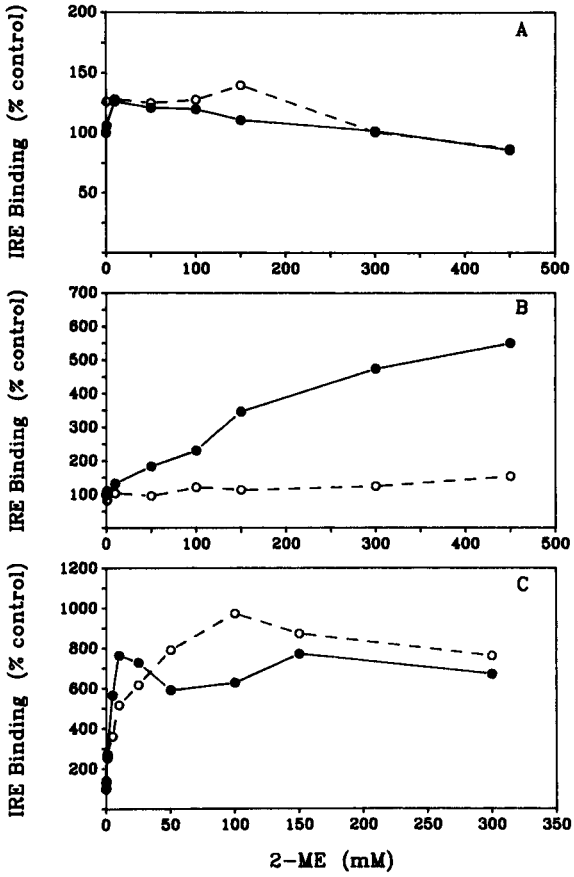

FIGURE 3: Effects of 2-mercaptoethanol on RNA binding by forms of IRP1. The effect of increasing concentrations of 2-mercaptoethanol on RNA binding activity of reduced apo-IRP1 (A), holo-IRP1 (B), and oxidized apo-IRP1 (C) was determined by gel shift assay. The various preparations of IRP1 were diluted to 0.1 nM (reduced IRP1) or 1.0 nM (c-aconitase and oxidized IRP1) and incubated in the presence of the indicated concentration of 2-ME and 1.0 nM ^{32}P-labeled IRE RNA from the first 70 nt of the rat L-ferritin 5′UTR for 10 min. Heparin (0.45 mg/mL final concentration) was added for 5 min, and then the free and bound RNA were separated by nondenaturing gel electrophoresis. Sodium citrate (pH 7.5) was added at 1 mM to the proteins before addition of 2-ME. Data are representative of results obtained with four to five separate experiments. Incubations with 2-ME in the presence of sodium citrate are indicated by the dotted line and open symbol (○), and incubations with 2-ME in the absence of sodium citrate are indicated by the solid line and filled symbol (●).

binding function (Haile et al., 1992b). Addition of increasing levels of 2-ME activated the RNA binding activity of c-aconitase such that at 450 mM a 5.5-fold increase was observed. In the presence of this level of 2-ME, 42% of the protein bound RNA, a capacity somewhat higher than that observed by reduced IRP1. As noted by others (Haile et al., 1992b), citrate completely eliminated the ability of 2-ME to activate the RNA binding function of c-aconitase (Figure 3B) but failed to significantly affect the response of IRP1 to 2-ME (Figure 3A). Thus, these preparations of the binding protein, highly purified c-aconitase and the reduced apoprotein derived from it by removal of the iron sulfur cluster, represent the two functionally opposing forms of IRP1, metabolic enzyme or high-affinity RNA binding protein.

Destruction of the Fe-S cluster present in aconitases by addition of a molar excess of ferricyanide and EDTA results in formation of oxidized forms of these proteins due to the presence of di- and polysulfides, some of which are likely to include Cys residues that were involved in ligation of the Fe-S cluster to the protein (Haile et al., 1992b; Kennedy et al., 1983). Recent evidence suggests that inactive species of IRP1, possibly containing di- or polysulfides, may have increased abundances in cells or cell extracts responding to oxidative stress (Cairo et al., 1995, 1996). Disulfide bond formation between Cys 437 and either Cys 503 or 506 impairs RNA binding by IRP1 (Hirling et al., 1994). We found that oxidized IRP1 binds IRE RNA with lower affinity ($K_D = 4.2 \pm 0.53$ nM) and binding capacity ($B_{max} = 0.67 \pm 0.21$) as compared to reduced apo-IRP1 (Figure 2C). RNA binding by oxidized IRP1 was greatly stimulated by 1−10 mM 2-ME, and citrate failed to influence the 2-ME effect (Figure 3C). Binding of IRE RNA to oxidized IRP1 was inhibited by addition of a specific competitor RNA (IRE RNA), whereas equimolar amounts of tRNA were without effect (results not shown).

The kinetics of phosphorylation of reduced IRP1 and c-aconitase by PKC were determined (Figure 4). At all time points examined, reduced IRP1 was a much-preferred

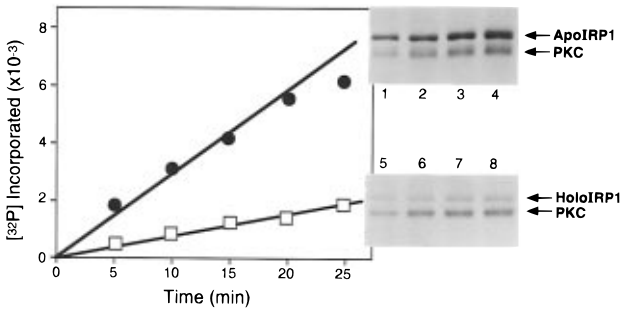

FIGURE 4: Comparison of c-aconitase and reduced IRP1 as substrates for protein kinase C. The c-aconitase (holo-IRP) or reduced IRP1 (apo-IRP1) form of IRP1 (5 μg) was phosphorylated with protein kinase C (2.7 units) in 50 μL reaction mixtures as previously described (Tuazon et al., 1989). Aliquots (40 μL) were withdrawn at designated time points, and 10 μL of 100 mM ATP and 20 μL of Laemmli sample buffer were added to stop the reaction. Samples were analyzed by SDS−PAGE, and the gel was stained with Coomassie brillant blue, destained, and dried. Incorporation of ^{32}P was quantitated by scintillation counting.

substrate for PKC. Overall, the rate of phosphorylation of reduced IRP1 was 4−5-fold higher than that observed for c-aconitase (Figure 4). These results agree with those obtained during purification of rat liver IRP1 where the apoprotein was the preferred substrate for PKC (Figure 1, lane 8) as compared to the DEAE-NA form which exhibited characteristics of the [3Fe-4S] species of IRP1 (Figure 1, lane 9). Phosphorylation of oxidized apo-IRP1 was not determined because of the requirement for 2-ME in the protein kinase assay.

Structural Differences in IRP1 as a Function of Iron-Sulfur Cluster Status. Our observations indicate that the presence or absence of the Fe-S cluster or the oxidation state of certain cysteines in the apoprotein influences RNA binding and/or phosphorylation potential. It has been suggested, but not directly demonstrated, that the RNA binding and aconitase forms of IRP1 exhibit significant differences in their structures (Barton et al., 1990; Hentze et al., 1989; Hirling et al., 1994; Kennedy et al., 1992; Klausner et al., 1993, 1994). We used proteases as probes of potential structural differences between reduced IRP1 and c-aconitase. Limited proteolysis has been used to define various structural aspects of nucleic acid binding proteins, including IRP1 (Swenson & Walden, 1994; Beekman et al., 1993; Keidel et al., 1994).

First, we compared the sensitivity to proteolysis and the resulting digestion pattern of the reduced IRP1 and the c-aconitase forms of the protein. Proteases that cleave after basic (endo Arg-C, thrombin), acidic (endo Glu-C), or hydrophobic (chymotrypsin) residues were chosen. Reduced IRP1 (lanes labeled A in Figure 5) was reproducibly cleaved by all of the proteases tested. Endo Lys-C cleaved reduced IRP1, producing two fragments with molecular weights of approximately 16 000 and 80 000 (Figure 5, lane 3, bands b and a). Endo Arg-C produced at least three bands with M_rs of approximately 85 000, 60 000, and 40 000 (Figure 5, lane 6, bands c−e). A lower-molecular weight fragment (M_r = 10 000) was observed on higher-percentage acrylamide gels (results not shown). Thrombin produced a cleavage pattern with reduced IRP1 identical to that obtained with endo Arg-C (results not shown). Endo Glu-C produced two fragments from reduced IRP1 with M_rs of approximately 65 000 and 30 000 (Figure 4, lane 8, bands f and g). Longer incubation times or higher concentrations of protease produced more

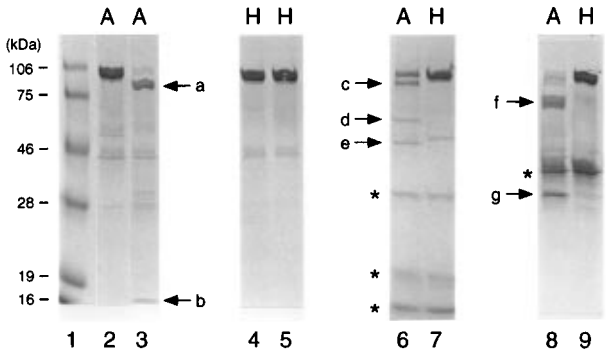

FIGURE 5: Sensitivity of reduced IRP1 and c-aconitase to the action of various proteases. Reduced IRP1 and c-aconitase were subjected to limited digestion by several proteases for 1, 5, 10, or 30 min as described in Materials and Methods. Each reaction mixture contained 4 μg of reduced IRP1 (A) or c-aconitase (H). Reactions were terminated by the addition of Laemmli sample buffer and the mixture denatured and then subjected to SDS−PAGE. The figure depicts the Coomassie-stained gels from specific time points: lane 1, molecular weight markers; lane 2, undigested IRP1 (apoprotein, A); lane 3, IRP1 incubated with endo Lys-C [1.75 μg (260 mu)/(μg of IRP1)] for 30 min; lane 4, undigested c-aconitase (holoprotein, H); lane 5, c-aconitase incubated with endo Lys-C for 30 min with the same concentration of protease as used with the apoprotein; lane 6, IRP1 incubated with endo Arg-C [1.25 μg/(μg of IRP1)] for 10 min; lane 7, c-aconitase incubated with endo Arg-C for 10 min with the same concentration of protease as used with the apoprotein; lane 8, IRP1 incubated with endo Glu-C [1.25 μg (275 mu)/(μg of IRP1)] in 40 mM ammonium bicarbonate (pH 7.8) and 7 mM 2-ME for 1 min; lane 9, c-aconitase incubated with endo Glu-C for 10 min. Arrows labeled a−g indicate the position of proteolytic fragments of IRP1. Polypeptides identified by an asterisk (*) indicate the position of migration of either endo Arg-C (lane 6) or endo Glu-C (lane 8).

extensive digestion of reduced IRP1 (results not shown). c-Aconitase was more resistant to proteolysis, and under the conditions used here, no cleavage was seen (Figure 4, compare lane 4 with lanes 5, 7 and 9).

Second, to address the relative sensitivity of reduced IRP1 and c-aconitase to limited proteolysis, a kinetic analysis was performed on these forms of the binding protein using chymotrypsin. Chymotrypsin caused a rapid reduction in the amount of intact reduced IRP1 and increased accumulation of several degradation products (Figure 6, panels B and C). After 15 s, three degradation products were observed: fragment b ($M_r \approx 68\,000$), fragment c ($M_r \approx 56\,000$), and fragment d ($M_r \approx 41\,000$) (Figure 6, panel B, lane 2). On some gels with a higher resolving power, fragment d was composed of a doublet (results not shown). Fragment e ($M_r \approx 30\,000$) was faintly visible at the first time point (Figure 6, panel B, lane 2). Fragment c decreased in intensity with time, whereas fragments d−f appeared to be more stable intermediates as their levels increased in intensity for at least 10 min after addition of protease (Figure 6, panel B, lanes 3−8). Fragment f was faintly present at early digestion times and increased in intensity as the incubation progressed (Figure 6, panel A, lanes 2−9). In contrast to what we observed for reduced IRP1, c-aconitase was not digested by chymotrypsin under these conditions (Figure 6, panels A and C). However, higher levels of chymotrypsin resulted in digestion of the c-aconitase form, and the pattern of digestion products differed greatly from that produced with IRP1 (results not shown).

Localization of Chymotrypsin Cleavage Sites in Reduced IRP1. To determine which regions of bovine-reduced IRP1

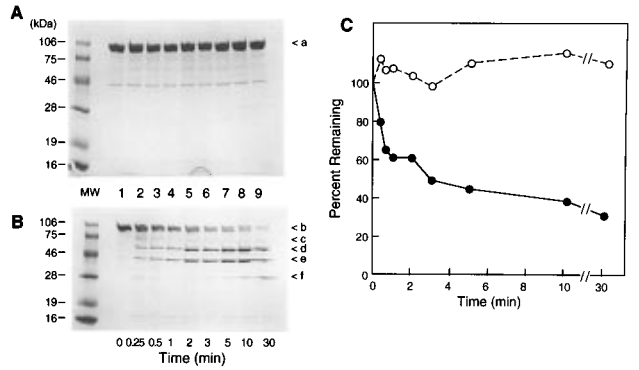

FIGURE 6: Effect of iron-sulfur cluster status on the kinetics of digestion of IRP1 by chymotrypsin. The c-aconitase or reduced IRP1 form of bovine IRP1 was incubated with chymotrypsin [150 ng of protease/(μg of protein)] for 0, 0.25, 0.5, 1, 2, 3, 5, 10, and 30 min. Each reaction mixture contained 4 μg of reduced IRP1 or c-aconitase. Reactions were terminated by the addition of Laemmli sample buffer and the mixture denatured at 100 °C for 5 min and then subjected to SDS−PAGE. Panel A depicts incubations of the c-aconitase form of the binding protein. Panel B depicts reactions containing the reduced IRP1 form of the binding protein. Lane MW is protein molecular weight markers: lane 1, no protease; lane 2, 0.25 min; lane 3, 0.5 min; lane 4, 1 min; lane 5, 2 min; lane 6, 3 min; lane 7, 5 min; lane 8, 10 min; and lane 9, 30 min. Panel C shows the amount of intact protein remaining at various times after addition of protease to the c-aconitase (○) or reduced IRP1 (●) form of the binding protein. The amount of intact protein remaining was determined by densitometric scanning of the Coomassie-stained gels using a computerized densitometer and Image One software (PDI).

Table 2: N-Terminal Sequence of Peptides Obtained after Limited Proteolysis of IRP1 with Chymotrypsin

peptide[a]	M_r	amino-terminal sequence	deduced sequence	predicted size	residue range
e-1	41	T-IGNSGPLP[b]	TCIGNSGPLP	42.8	505−889
e-2	41	NRRADS	NRRADS	40.8	133−504
f	30	NALAAP-DKL[c]	NALAAPSDKL	30	624−889

[a] This refers to peptides observed in chymotryptic digests as shown in Figure 6. [b] The second residue in this sequence was likely a Cys as the peak representing the form of Cys covalently modified by acrylamide monomer was observed in this cycle (Perkin-Elmer/Applied Biosystems User Guide 61). [c] The seventh cycle in this sequence was not assignable to a specific amino acid.

become accessible to proteolysis upon loss of the iron-sulfur cluster, chymotryptic digestion products of IRP1 were sequenced. Fragment e (p41) from the chymotrypsin digestion of reduced IRP1 contained two polypeptides with N termini at residues 133 and 505 (Table 2), indicating cleavages after residues 132 and 504, respectively. On the basis of sequence homology with m-aconitase, residue 132 should be near the entrance to the putative cleft and residue 504 should be within the putative cleft. Since the full-length sequence of bovine IRP1 is not available, a comparison was made to the human, rabbit, rat, and mouse IRP1 proteins, which are 98% identical (Hirling et al., 1992; Patino & Walden, 1992; Philpott et al., 1991; Rouault et al., 1990, 1992; Yu et al., 1992). Fragment e-1 has a predicted molecular weight of 42 813 based on the rabbit IRP1 sequence and should span residues 505−889. Fragment e-2 has a predicted molecular weight of 40 753 and should span residues 133−504. Fragment f has an N terminus at residue 624 and a predicted molecular weight of 29 500 and should span residues 624−889. Residue 624 is predicted

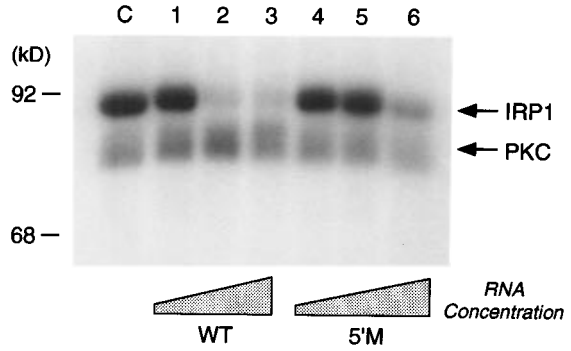

FIGURE 7: Specific inhibition of IRP1 phosphorylation by IRE containing RNA. Reduced IRP1 (0.9 μg of protein) was phosphorylated by PKC in the presence or absence of RNA for 15 min at 30 °C. Phosphorylation reaction mixtures were analyzed by SDS−PAGE. Lane C was with control, and no RNA added. ^{3}H-labeled wild type rat L-ferritin IRE RNA was added to incubations in lanes 1−3 as follows: lane 1, 0.01 μM; lane 2, 0.1 μM; and lane 3, 1 μM. The secondary structure mutant of the rat L-ferritin IRE was added to incubations in lanes 4−6 at the following concentrations: lane 4, 0.01 μM; lane 5, 0.1 μM; and lane 6, 1 μM. The counts per minute incorporated into IRP1 for lanes 1−7 was 730, 750, 120, 110, 680, 630, and 250, respectively. The arrows indicate the position of ^{32}P-labeled IRP1 phosphorylated by PKC or autophosphorylated PKC.

to lie in the proposed hinge linker of IRP1 (Swenson & Walden, 1994; Rouault et al., 1992). Other than residues 628 and 631, the peptide sequences reported in Table 2 for bovine IRP1 are identical to those reported for the deduced sequence of IRP1 from human, rabbit, rat, and mouse (Hirling et al., 1992; Patino & Walden, 1992; Philpott et al., 1991; Rouault et al., 1990, 1992; Yu et al., 1992). In human IRP1, residue 628 is Thr, and for murine IRP1, residue 631 is a Glu.

IRE RNA Specifically Inhibits PKC-Dependent Phosphorylation of IRP1. To further investigate the extent to which RNA binding and phosphorylation sites may lie in the same or overlapping regions of IRP1, we examined the effect of IRE-containing RNA on phosphorylation of the binding protein. We tested the effect of an IRE-containing RNA composed of the first 73 nt of rat L-ferritin 5′UTR and a mutant form of this RNA in which the 5′ side of the upper stem of the IRE was mutated (5′M IRE). Compared to the wild type rat L-ferritin 5′UTR RNA, the 5′M RNA contains a significantly different secondary structure due to disruption of base-pairing capacity in the upper stem region and binds less well to IRP1 (Bettany et al., 1992). For the *in vitro* phosphorylation assays, it is necessary to use approximately 0.5−1 μg of IRP1. In these experiments, we used 0.9 μg of reduced IRP1 which in the kinase assay is a concentration of 0.18 μM. Because of this requirement, the binding of RNA to IRP1 does not occur under equilibrium conditions. One of two RNAs was added to the kinase reaction at final concentrations of 0.01, 0.1, and 1 μM. Wild type IRE RNA inhibited phosphorylation significantly at 0.1 and 1 μM (Figure 7, lanes 2 and 3). In contrast, the RNA containing the mutated IRE (5′M) was a less efficient inhibitor of phosphorylation than was the wild type IRE; at 0.1 μM, little or no inhibition was obtained, and at 1 μM, only partial inhibition was apparent (Figure 7, lanes 5 and 6). Neither RNA greatly affected the autophosphorylation activity of PKC (Figure 7) or the ability of the kinase to phosphorylate a control protein further, indicating the specific

effect of IRE-containing RNA on the phosphorylation of IRP1 (results not shown).

DISCUSSION

It has been hypothesized that cluster-dependent alterations in RNA binding occur, at least in part, due to alterations in the extent to which the putative cleft in IRP1 is open and accessible for interaction with the IRE (Hirling et al., 1994; Klausner et al., 1993, 1994). While previous studies demonstrated that certain amino acids within the proposed cleft of IRP1 have mutually exclusive roles in RNA binding or enzymatic function, little evidence is available regarding the nature and extent of structural rearrangements in the binding protein as a function of the presence or absence of the cluster (Hirling et al., 1994; Klausner et al., 1993, 1994; Philpott et al., 1993, 1994). These studies have provided results that are consistent with the proposal that the putative cleft in IRP1 serves as a common locus for the two functions of the protein (Hirling et al., 1994; Klausner et al., 1994; Philpott et al., 1993, 1994). Our results provide direct evidence for significant structural differences between the reduced IRP1 and c-aconitase forms of the binding protein. We observed that, when the Fe-S cluster is chemically removed, there is a 20-fold increase in RNA binding affinity. Concomitantly, we demonstrated an increased accessibility of reduced IRP1 to the action of several proteases. Our results provide support for previous suggestions that the iron status of the cell can induce structural alterations in IRP1 (Barton et al., 1990; Hentze et al., 1989).

To provide a more detailed description of these iron-dependent changes in the structure of IRP1, we sequenced chymotryptic fragments of the apoprotein. First, we identified two regions, involved in RNA binding and/or its regulation, predicted to be near (residue 132) or within (residue 504) the putative cleft of IRP1 that become accessible to chymotrypsin when the Fe-S cluster is removed from the c-aconitase form. Much interest has been expressed concerning what regions of IRP1 are necessary for high-affinity interaction with RNA, and several studies have identified residues in the region 116−151 (Basilion et al., 1994; Neupert et al., 1995; Swenson & Walden, 1994). Our observation of chymotryptic cleavage after residue 132, in reduced IRP1 but not in c-aconitase, provides a direct demonstration that the absence of cluster results in increased accessibility of a region of the protein essential for high-affinity RNA binding. Residues 480−623 (Swenson & Walden, 1994) as well as residues near the C terminus (Hirling et al., 1992) also appear to contribute to RNA binding by IRP1. Residues 480−623 contain Cys 503 and Cys 506 which are essential for iron regulation of RNA binding and also are predicted to be on the surface of the putative cleft of IRP1 (Hirling et al., 1994; Philpott et al., 1993, 1994; Swenson & Walden, 1994). It is of interest therefore that we observed cleavage after residue 504 which suggests that residues within the putative cleft of IRP1 become accessible to chymotrypsin after removal of the cluster from c-aconitase. Taken together, our results indicate that on removal of the Fe-S cluster residues involved in RNA binding and its regulation become more accessible for interaction with RNA or other factors.

Second, by demonstrating chymotryptic cleavage between residues 623 and 624 of reduced IRP1, but not of c-aconitase, our results indicate that loss of cluster affects accessibility of the putative hinge linker region of IRP1 to chymotrypsin. A similar conclusion can be inferred from the results obtained with endo Glu-C. Hirling et al. (1992) found using the RNA binding form of human IRP1 that endo Glu-C cleaved at residue 621, also within the hinge linker region. We found that c-aconitase was not affected by endo Glu-C under conditions where reduced IRP1 was cleaved into two fragments of a size similar to that observed by Hirling et al. (1992). On the basis of the structure of m-aconitase, the hinge linker of IRP1 should be on an opposite face of the protein as compared to the cleft (Klausner et al., 1994; Robbins & Stout, 1989). Thus, our results support the concept that loss of the Fe-S cluster results in structural alterations in both the putative cleft and hinge linker regions of the binding protein.

Third, in the comparison of the apo and holo forms of the binding protein, a 4−5-fold difference in the rate of phosphate incorporation was apparent, with apo-IRP1 being the preferred substrate for PKC. Thus, the presence of the Fe-S cluster results in structural alterations in IRP1 which reduces accessibility of the PKC phosphorylation sites. It is of particular interest that the chymotryptic cleavage site between residues 132 and 133 becomes accessible after removal of cluster, providing evidence that Ser 138 may also exhibit cluster-dependent changes in its accessibility. These results, coupled with the observation that IRE RNA specifically inhibits PKC-dependent phosphorylation, provide additional support for our previous suggestion that the sites at which PKC acts are near the entrance to the putative cleft in the binding protein (Eisenstein et al., 1993).

Finally, phosphorylation appears to have differing effects on IRP1 and IRP2. We previously demonstrated that phosphorylation affects IRP2 function through an oxidation−reduction mechanism wherein phosphorylation increased the proportion of the protein in the reduced or RNA-binding state (Schalinske & Eisenstein, 1996). Our current observations support our previous hypothesis that PKC-dependent phosphorylation of IRP1 serves as a means of partitioning the protein between its two opposing functions. This concept is supported by the fact that Ser 138 is within one region of IRP1 known to be important for RNA binding (residues 116−151) (Neupert et al., 1995) and near another region that is apparently essential for the aconitase function (residues 125 and 126) (Rouault et al., 1992). Thus, phosphorylation at Ser 138 may selectively affect the ability of these residues to support the separate functions of IRP1. Given the preferential phosphorylation of the apoprotein by PKC, it seems reasonable to speculate that phosphorylation may block or inhibit cluster assembly or alter certain properties of the cluster, possibly including altering its stability. In this manner, phosphorylation may alter the set point at which iron affects IRP1 function. We are currently testing these hypotheses by examining the effects of phosphorylation on *in vitro* reconstitution of cluster as well as by structure−function analysis of recombinant species of IRP1 mutagenized in the phosphorylation sites.

ACKNOWLEDGMENT

We thank Helmut Beinert for helpful discussions and comments on the manuscript, Jolinda Traugh, William

Walden, and Dave Stout for stimulating discussions, and Dan Steffen for excellent technical assistance.

REFERENCES

Barton, H. A., Eisenstein, R. S., Bomford, A. B., & Munro, H. N. (1990) *J. Biol. Chem. 265*, 7000−7008.

Basilion, J. P., Rouault, T. A., Massinople, C. M., Klausner, R. D., & Burgess, W. H. (1994) *Proc. Natl. Acad. Sci. U. S. A. 91*, 574−578.

Beekman, J. M., Allan, G. F., Tsai, S. Y., Tsai, M.-J., & O'Malley, B. W. (1993) *Mol. Endocrinol. 7*, 1266−1274.

Beinert, H., & Thomson, A. J. (1983) *Arch. Biochem. Biophys. 222*, 333−361.

Beinert, H., & Kennedy, M. C. (1993) *FASEB J. 7*, 1442−1449.

Bettany, A. J. E., Eisenstein, R. S., & Munro, H. N. 1992. *J. Biol. Chem. 267*, 16531−16537.

Cairo, G., Tacchini, L., Pogliaghi, G., Anzon, E., Tomasi, A., & Bernelli-Zazzera, A. (1995) *J. Biol. Chem. 270*, 700−703.

Cairo, G., Castrusini, E., Minotti, G., & Bernelli-Zazzera, A. (1996) *FASEB J. 10*, 1326−1335.

Eisenstein, R. S., Tuazon, P. T., Schalinske, K. L., Anderson, S. A., & Traugh, J. A. (1993) *J. Biol. Chem. 268*, 27363−27370.

Eisenstein, R. S., Kennedy, M. C., & Beinert, H. (1997) in *Metal Ions and Gene Regulation* (Silver, S., & Walden, W., Eds.) Chapman and Hall, New York (in press).

Emery-Goodman, A., Hirling, H., Scarpellino, L., Henderson, B., & Kühn, L. C. (1993) *Nucleic Acids Res. 21*, 1457−1461.

Guo, B., Yu, Y., & Leibold, E. A. (1994) *J. Biol. Chem. 269*, 24252−24260.

Guo, B., Phillips, J. D., Yu, Y., & Leibold, E. A. (1995) *J. Biol. Chem. 270*, 21645−21651.

Haile, D. J., Rouault, T. A., Tang, C. K., Chin, J., Harford, J. B., & Klausner, R. D. (1992a) *Proc. Natl. Acad. Sci. U.S.A. 89*, 7536−7540.

Haile, D. J., Rouault, T. A., Harford, J. B., Kennedy, M. C., Blondin, G. A., Beinert, H., & Klausner, R. D. (1992b) *Proc. Natl. Acad. Sci. U.S.A. 89*, 11735−11739.

Hentze, M. W., & Argos, P. (1991) *Nucleic Acids Res. 19*, 1739−1740.

Hentze, M. W., & Kühn, L. C. (1996) *Proc. Natl. Acad. Sci. U.S.A. 93*, 8175−8182.

Hentze, M. W., Rouault, T. A., Harford, J. B., & Klausner, R. D. (1989) *Science 244*, 357−359.

Hirling, H., Emery-Goodman, A., Thompson, N., Neupert, B., Seiser, C., & Kühn, L. C. (1992) *Nucleic Acids Res. 20*, 33−39.

Hirling, H., Henderson, B. R., & Kühn, L. C. (1994) *EMBO J. 13*, 453−461.

Iwai, K., Klausner, R. D., & Rouault, T. A. (1995) *EMBO J. 14*, 5350−5357.

Kaptain, S., Downey, W. E., Tang, C., Philpott, C., Haile, D., Orloff, D. G., Harford, J. B., Rouault, T. A., & Klausner, R. D. (1991) *Proc. Natl. Acad. Sci. U.S.A. 88*, 10109−10113.

Keidel, S., LeMotte, P., & Apfel, C. (1994) *Mol. Cell. Biol. 14*, 287−294.

Kennedy, M. C., Emptage, M. H., Dreyer, J. L., & Beinert, H. (1983) *J. Biol. Chem. 258*, 11098−11105.

Kennedy, M. C., Mende-Mueller, L., Blondin, G. A., & Beinert, H. (1992) *Proc. Natl. Acad. Sci. U.S.A. 89*, 11730−11734.

Klausner, R. D., Rouault, T. A., & Harford, J. B. (1993) *Cell 72*, 19−28.

Klausner, R. D., Stout, C. D., & Rouault, T. A. (1994) *Chem. Biol.* (Introductory Issue), xiv−xv.

Laemmli, U. K. (1970) *Nature 227*, 680−685.

Müllner, E. W., Neupert, B., & Kühn, L. C. (1989) *Cell 58*, 373−382.

Neupert, B., Thompson, N. A., Meyer, C., & Kühn, L. C. (1990) *Nucleic Acids Res. 18*, 51−55.

Neupert, B., Menotti, E., & Kühn, L. C. (1995) *Nucleic Acids. Res. 14*, 2579−2583.

Pantopoulos, K., Gray, N., & Hentze, M. W. (1995) *RNA 1*, 155−163.

Patino, M. M., & Walden, W. E. (1992) *J. Biol. Chem. 267*, 19011−19016.

Philpott, C. C., Rouault, T. A., & Klausner, R. D. (1991) *Nucleic Acids Res. 19*, 6333.

Philpott, C. C., Haile, D., Rouault, T. A., & Klausner, R. D. (1993) *J. Biol Chem. 268*, 17655−17658.

Philpott, C. C., Klausner, R. D., & Rouault, T. A. (1994) *Proc. Natl. Acad. Sci. U.S.A. 91*, 7321−7325.

Robbins, A. H., & Stout, C. D. (1989) *Proteins 5*, 289−312.

Rouault, T. A., Hentze, M. W., Haile, D. J., Harford, J. B., & Klausner, R. D. (1989) *Proc. Natl. Acad. Sci. U.S.A. 86*, 5768−5772.

Rouault, T. A., Tang, C. K., Kaptain, S., Burgess, W. H., Haile, D. J., Samaniego, F., McBride, O. W., Harford, J. B., & Klausner, R. D. (1990) *Proc. Natl. Acad. Sci. U.S.A. 87*, 7958−7962.

Rouault, T. A., Stout, C. D., Kaptain, S., Harford, J. B., & Klausner, R. D. (1991) *Cell 64*, 881−883.

Rouault, T. A., Haile, D. J., Downey, W. E., Philpott, C. C., Tang, C., Samaniego, F., Chin, J., Paul, I., Orloff, D., Harford, J. B., Hentze, M. W., & Klausner, R. D. (1992) *Biometals 5*, 131−140.

Samaniego, F., Chin, J., Iwai, K., Rouault, T. A., & Klausner, R. D. (1994) *J. Biol. Chem. 269*, 30904−30910.

Schalinske, K. L., & Eisenstein, R. S. (1996) *J. Biol. Chem. 271*, 7168−7176.

Swenson, G. R., & Walden, W. E. (1994) *Nucleic Acids Res. 22*, 2627−2633.

Theil, E. C. (1994) *Biochem. J. 304*, 1−11.

Tuazon, P. T., Merrick,W. C., & Traugh, J. A. (1989) *J. Biol. Chem. 264*, 2773−2777.

Walden, W. E., Patino, M. M., & Gaffield, L. (1989) *J. Biol. Chem. 264*, 13765−13769.

Yu, Y., Radisky, E., & Leibold, E. A. (1992) *J. Biol. Chem. 267*, 19005−19010.

BI9624447